Review Article/ Mechanical Engineering, Mechatronics, and Materials Science https://doi.org/10.15446/ing.investig.93710

Soil Biodegradation of a Blend of Cassava Starch and Polylactic Acid

Biodegradación en suelo de una mezcla de almidón de yuca y ácido poliláctico

Margarita R. Salazar-Sánchez[1], Laura I. Delgado-Calvache[2], Juan C. Casas-Zapata[3], Héctor S. Villada-Castillo[4] and Jose F. Solanilla-Duque[5]

ABSTRACT

This study evaluated bio-based blended films produced from polylactic acid (PLA) and thermoplastic starch (TPS) under soil conditions for four weeks (W). The degradation of the film was evaluated in addition to thermal, structural, and morphological changes on the surface of the material. There were evident structural changes; the TPS present in the film degraded from weeks 0 to 4, exhibiting a loss of mass between 350 and 365 ˚C in the TGA test. This behavior was attributed to the condensation of hydroxyl groups of the cassava starch as well as to a loss of mass corresponding to the degradation of PLA between 340 and 350 ˚C. The addition of TPS in the PLA-containing matrix resulted in a decrease in the Tg of the PLA/TPS blends. The increase in crystallinity improved the water vapor permeability in the structure. Consequently, the incorporation of starch in these blends not only reduces the cost of the material, but it also contributes to its rapid biodegradation (68%). These results contribute and offer new alternatives to accelerate the biodegradation process of biomaterials.

Keywords: disintegration, packing, biopolymers, soil, TPS/PLA

RESUMEN

Este estudio evaluó películas de mezcla de base biológica producidas a partir de ácido poliláctico (PLA) y almidón termoplástico (TPS) bajo condiciones en suelo durante cuatro semanas (W). Se evaluó la degradación de la película, además de los cambios térmicos, estructurales y morfológicos de la superficie del material. Hubo cambios estructurales evidentes; el TPS presente en la película se degradó desde la semana 0 hasta la 4, mostrando una pérdida de masa entre 350 a 365 ˚C en la prueba de TGA. Este comportamiento se atribuyó a la condensación de grupos hidroxilos del almidón de yuca y a una pérdida de la masa correspondiente a la degradación del PLA entre 340 a 350 ˚C. La adición de TPS en la matriz que contiene PLA dio lugar a una disminución en la Tg de las mezclas de PLA/TPS. El incremento de la cristalinidad mejoró la permeabilidad al vapor de agua en la estructura. Por lo tanto, la incorporación de almidón en estas mezclas no solo reduce el coste del material, sino que también contribuye a su rápida biodegradación (68%). Estos resultados contribuyen y ofrecen nuevas alternativas para acelerar el proceso de biodegradación de los biomateriales.

Palabras clave: desintegración, empaque, biopolímeros, suelo, TPS/PLA

Received: February 17th, 2021
Accepted: March 09th, 2022

Introduction

Polymers derived from plant feedstocks are increasingly replacing plastic materials, reducing their environmental impact (S. Lambert and Wagner, 2017; T. Lambert and Perga, 2019; Mierzwa-Hersztek et al., 2019). Polymers of industrial interest include cellulose, starch, alginic acids, natural polypeptides such as gelatins, and bacterial polyesters (Heidemann et al., 2019). The biodegradation of contaminated plastics under composting conditions has been reported as an effective method to reduce plastic contamination (Bher *et al.*, 2019). However, biodegradable polymers offer the possibility of reducing the environmental impact of chemical waste from landfills, which is due to their degradation speed under composting conditions at the site of final disposal (Castro-Aguirre et al., 2018). However, some biodegradable polymers such as polylactic acid (PLA) do not biodegrade as quickly as other organic waste during composting (Lv, Zhang, et al., 2017), since their degradation depends on

[1] Biologist, Universidad del Cauca; PhD in Agricultural and Agroindustrial Sciences, Universidad del Cauca. Affiliation: Assistant professor, Agro-industrial Engineering Area, Department of Engineering and Technology, Universidad Popular del Cesar, Valledupar, Colombia. Email: mdelrosariosalazar@unicesar.edu.co

[2] Environmental engineer. Affiliation: Young researcher, Universidad del Cauca, Popayán, Colombia. Email: laurita@unicauca.edu.co

[3] Chemical engineer, Universidad de Antioquia; PhD in Engineering, Universidad de Antioquia, Medellín, Colombia. Affiliation: Full professor, Environmental and Sanitary Engineering Area, Department of Civil Engineering, Universidad del Cauca, Popayán, Colombia. Email. jccasas@unicauca.edu.co

[4] Agro-industrial engineer, Universidad La Gran Colombia, Bogotá, Colombia; Ph.D. in Engineering, Universidad del Valle, Cali, Colombia. Affiliation: Full professor, Agro-industry Area, Department of Agricultural Sciences, Universidad del Cauca, Popayán, Colombia. Email: villada@unicauca.edu.co

[5] Agro-industrial engineer, Universidad La Gran Colombia, Bogotá, Colombia; Ph.D. in Science and Technology: Colloids and Interfaces, Universidad Pablo De Olavide, Sevilla, Spain. Affiliation: Associate professor, Agro-industry area, Department of Agricultural Sciences, Universidad del Cauca, Popayán, Colombia. jsolanilla@unicauca.edu.co

How to cite: Salazar-Sánchez, M. R., Delgado-Calvache, L. I., Casas-Zapata, J. C., Villada-Castillo, H. S., and Solanilla-Duque, J. F. (2022). Soil biodegradation of a blend of cassava starch and polylactic acid. *Ingeniería e Investigación, 42*(3), e93710. https://doi.org/10.15446/ing.investig.93710

the action of microorganisms (Pattanasuttichonlakul et al., 2018) and hydrolysis reactions that can break lactic acid chain monomers into smaller molecules such as lactide. Consequently, the low degradability of PLA has affected its general acceptance in industrial composting. Blends of PLA with other biomolecules such as corn starch have been widely documented (Shogren et al., 2003), and blends of 4032D PLA with cassava starch (TPS) have been reported in recent years for packaging and food service applications. In these compounds, due to the effect of biodegradation, each of the components is converted into biomass, which returns to the environment in the form of carbon dioxide (CO_2), methane (CH_4), and water. During this process, the polymer or blend undergoes structural changes implying the loss of mechanical properties due to disintegration, fragmentation, and mineralization (Salazar-Sánchez et al., 2020). The objective of this work was to study the biodegradation of a blend of cassava starch and PLA under natural environmental conditions.

Materials and methods

Sample preparation

The plastic film was produced in the rheology laboratory of Universidad del Cauca. The film is a polymer obtained from renewable sources such as cassava starch (*Manihot esculenta* Crantz) and PLA. Three films were used: a film of thermoplastic starch from Cassava (TPS), a film of polylactic acid (PLA Ingeo 4032D, Mn = 88 500 g.mol^{-1}, Mw/Mn = 1,8), and one film product of a blend of the two compounds with a ratio of 72:28 (TPS-PLA) following the procedure described by Salazar-Sánchez et al. (2019).

Fourier transform spectrophotometry (ATR-FTIR) analysis

The tests were conducted in accordance with ASTM E1252-98 (ASTM International, 2013) via Fourier transform infrared spectroscopy (FT-IR) (IRAffinity-1S, Shimadzu, Inc., Shelton CT, Japan). A horizontal attenuated total reflectance (ATR) sampling accessory (ATR-8200HA) equipped with a ZnSe cell was employed for the measurement (Salazar-Sánchez et al., 2019).

Thermal properties

A thermogravimetric analysis (TGA) and a differential sweep analysis (DSC) were performed using a TGA (TGA 2050TA Instruments, USA) and a DSC (Q20 TA Instruments, New Castle, USA), respectively, according to ASTM E1131-20 and ASTM D3418-15 (ASTM International, 2015, 2020; Daza et al., 2018; Carmona et al., 2015; Frone et al., 2013).

Isotherm analysis

The sorption isotherms were determined at 10, 25, and 35 °C using a vapor sorption analyzer (Aqua Lab VSA, USA) with an a_w range of 0,5-0,95. The equilibrium moisture content on a dry basis was plotted against the a_w in order to obtain the equilibrium moisture curves (Dutcher et al., 2011). The performance of the models (Table 1) was evaluated via the adjusted coefficient of determination (R^2_{adj}) and mean square error (MSE). The models were selected on the basis of a high R^2_{adj} and a low MSE (Andrade et al., 2011; Arslan-Tontul, 2020; Homez et al., 2018; Iglesias and Chirife, 1995; Torres et al., 2012).

Biodegradation analysis

The biodegradability test was conducted in triplicate according to ASTM D5988 (ASTM International, 2018). A mixture of coffee soils and compost (derived from agricultural residues) was used as inoculum at a ratio of 25:1, and 4% sand was added as a structuring material to improve aeration. A physicochemical analysis of the soil was performed (organic carbon, water retention capacity, cation exchange capacity, capillary electrophoresis, pulse differential polarography, and carbon/nitrogen ratio) using the Colombian Technical Standard SSLMM-42-2-92 and the 3111B standard method (APHA, 1999) to determine metals and minerals. Microbiological properties were determined by counting the colony-forming units (CFC/g) of mesophylls, thermophiles, mold, yeast, *Nematodes* and/or *Protozoa*, *Enterobacteria,* and *Salmonella* (supplementary material).

Table 1. Water activity equation models

Model	Equation	Reference
Oswin	$X = a\left(\frac{a_w}{1-a_w}\right)^b$	Oswin (1946)
GAB	$\frac{X_m C k a_w}{\left[(1-ka_w)(1-ka_w+Cka_w)\right]}$	Guggenheim (1966), Anderson (1946), de Boer (1953), van den Berg (1981)
BET	$\frac{X_m C a_w}{\left[(1-a_w)+(C-1)((1-a_w)a_w)\right]}$	Brunauer et al. (1938), Aguerre et al. (1989)
Hasley	$X = \left(-\frac{a}{lna_w}\right)^{\frac{1}{b}}$	Halsey (1948)

Source: Authors

The moisture content was adjusted to approximately 63%. The test material was the mixture described above (TPS/PLA), and, as a reference microcrystalline, cellulose was used for thin-layer chromatography (Merck KgaA, Germany), as well as 4032D PLA (Ingeo). The cellulose and PLA were conditioned according to ISO 10210 (ISO, 2012), and the crushed fraction with a particle diameter between 250 and 125 µm was chosen. Each reactor was loaded with 200 g of inoculum and 0,74245 ± 0,0009 g of TPS/PLA, 0,6467 ± 0,0016 g cellulose, and 1,0028 ± 0,0005 g PLA –all samples on a wet basis. The carbon mineralization in the mixtures was quantified using a respirometry assembly in a closed chamber, where $Ba(OH)_2$*$8H_2O$ 0,025 N (Merck KgaA,

Germany) was used as CO_2 adsorbent, and HCL 0,05 N as titrator (Merck, Germany). The titration was performed at the endpoint of a 5 ml sample of adsorbent, aided by a TITRINO PLUS (Metrohm) automatic titrator. For the statistical evaluation of the results obtained from the biodegradation process of the samples studied for 4 weeks (W), a univariate analysis of variance was performed (ANOVA and Tukey tests with a 95% reliability and minimum significant difference) and the SMD (standardized mean difference) was estimated. The differences were considered to be significant when $p<0,05$.

Scanning electron microscopy (SEM) analysis

The samples were characterized via scanning electron microscopy (SEM) using a QUANTA 200F (FEI, The Netherlands). Each SEM sample was coated with Gold-Palladium (0,8 nm thick coating) in an EmiTech K575X Peltier Cooled (QuorumTech, United Kingdom). The samples were observed and analyzed at an accelerating voltage of 10,0 kV at different magnifications (from 50X to 2000X).

Results and discussions

ATR-FTIR analysis

The FTIR spectra were analyzed in the range of 400-4 000 cm^{-1} and are shown in Figure 1. Bands between 900 and 1 010 cm^{-1} indicate C-O-C bonds (Liu et al., 2011; Salazar-Sánchez et al., 2019). The characteristic peaks at 2 918 and 2 848 cm^{-1} correspond to CH_3, and those between 1 747 and 1 180 cm^{-1} are characteristic of 4032D PLA with C=O and C-O carbonyl group stretching, respectively (Riba et al., 2020). The peaks at 730 cm^{-1} are associated with the bending of the C=C group of the PLA's main chain. Flexure of the carbonyl group CH_3 was observed in the 1 458 and 1358 cm^{-1} peaks, and there was also a CH_3 shift in the 1 072 cm^{-1} peak. Stretching of the -C-COO (1 276 cm^{-1}) and C-O-C (872 cm^{-1}) groups was observed in the PLA spectrum. Similarly, vibrations corresponding to the stretching of the hydroxyl (O-H) group between the 3 400-2 400 cm^{-1} bands were seen.

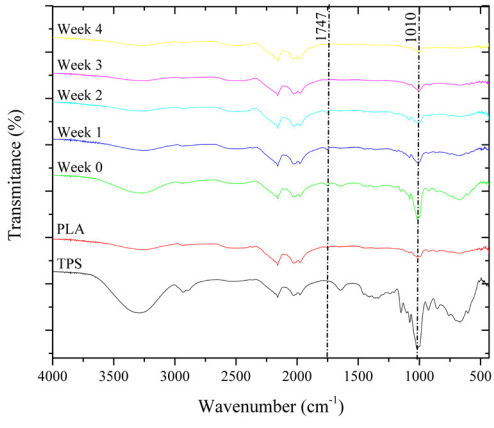

Figure 1. Fourier transform infrared (ATR-FTIR) spectra of the films
Source: Authors

Additionally, the spectra of TPS were compared because, when it blends with PLA, the mechanical, thermal, and other properties related to these mixtures (PLA/TPS) are modified. Therefore, the peaks to be analyzed were established between 750 and 1 250 cm^{-1} in order to understand the behavior of the TPS structure regarding its amylose/amylopectin composition before blending, as it is important to understand the crystalline and amorphous behavior of these molecules in the mixture. The stretching attributed to bands 1 040 cm^{-1} (C-O), 1 024 cm^{-1} (C-C), and 680 cm^{-1} (C-O-C) indicates a sensitivity to crystalline change. In other words, decreasing the crystallinity increases the 1 024 cm^{-1} band, whereas the intensity of the peak at 1 040 cm^{-1} increases with crystallinity, considering the crystalline structures of starch in this area (Cao et al., 2020). The intensity ratio between these two bands (1 046/1 024 cm^{-1}) is 1,72, thus indicating an increase in crystallinity in starch, which has a high degree of organization and is composed mainly of amylopectin (Özeren et al., 2020; Mierzwa-Hersztek et al., 2019; Homez et al., 2018; Nevoralová et al., 2019). The PLA/TPS film spectra show a stretch in the OH group in the region from 3 260 to 3 350 cm^{-1}. Likewise, the characteristic -CH peak of starch shows stretching in the 2 914 cm^{-1} band. The 1 024 cm^{-1} peak exhibited a shrinkage that could be due to starch retrogradation. When exposing the film to the biodegradation process, structural changes were evidenced; the TPS present in the film degraded from W0 to W4. These changes could be observed in the spectra and are attributed to changes in the crystallinity of starch, which is reflected by the glycosidic bonds of the TPS Neat and could be due to the fact that starch degradation occurs first in the amorphous region (amylose) as well as in the PLA, where the hydrogen bonds are very weak and more accessible to microorganisms, which degrades substantially faster compared to the crystalline part (Sedničková et al., 2018). The bands located at 1 040 cm^{-1} indicate a C-O functional group. The band located at 1 024 cm^{-1} indicates the amorphous region of starch given the presence of the C-C group. Similar observations were reported by Palai et al. (2019) and Wang et al. (2020), as well as at 680 cm^{-1} with vibrations for the C-O-C group (Gopi et al., 2019). The decrease in peak intensity at 1 178 cm^{-1} for PLA/TPS may be due to the weak chemical interaction between PLA and TPS (Muller et al., 2017).

Thermal properties

A loss of mass could be observed which reflected the condensation of hydroxyl groups (300-400 °C) (Figures 2a and b). The magnitude and location of this mass loss changed according to the degradation time (W0 to W4). In W1 and W2, the film showed a significant mass loss in the temperature range of 350-365 °C, which indicates the condensation of the hydroxyl groups of cassava starch. In W3 and W4, there was a mass loss in the range of 340-350 °C, which corresponds to the degradation of the PLA present in the blend. Similar results were reported by Nasseri et al. (2020) for mixtures of acetylated rice starch and PLA. The degradation temperatures decreased due to the

consumption of the starch content by the microorganisms (de Oliveira, Barbosa, et al., 2019; de Oliveira, de Oliveira Mota et al., 2019; Gralde, et al., 2019).

Table 2. Thermal data for PLA in their corresponding blends: samples (S), week (W), glass transition temperature (Tg), heat capacity (Cp), crystallization temperature (Tc), enthalpy of crystallization (ΔHc) melting temperature I (Tm), enthalpy of fusion (ΔHm), and crystallinity indices (Xc)

S	Tg (°C)	Cp J/g·°C	Tc (°C)	ΔHc (J/g)	Tm (°C)	ΔHm (J/g)	Xc (%)
W0	52,54	0,37	110,35	19,04	167,38	33,70	34,05
W1	56,75	0,38	109,35	18,82	167,64	31,28	33,97
W2	57,82	0,39	108,68	18,18	166,88	33,03	32,62
W3	61,18	0,39	117,93	20,83	169,65	24,81	25,84
W4	61,89	0,38	119,97	24,46	170,70	28,30	22,61
PLA W4	64,06	0,53	137,00	24,41	170,69	27,79	21,49
PLA	57,27	0,48	149,82	1,45	161,33	52,98	55,17
TPS	50,05	0,34	-	-	147	26,03	-

Source: Authors

The DSC curves show the glass transition (Tg), crystallization (Tc), and melting I (Tm) temperatures (Figure 3). The Tg is around 60 °C in the analyzed samples. It increases in W3 and W4 and has a lower value in W1 and W2, which could be due to the difference in the nature of the incidence of starch. The addition of TPS within the PLA matrix resulted in a decrease in the Tg of the PLA/TPS blends. A decrease in Tg increased the starch concentration (Li et al., 2020). This decrease in the Tg of the films can be attributed to the plastification of starch with glycerol, given the mobility of the chains caused by the migration of glycerol in the dispersed phase of TPS (Özeren et al., 2020). This effect is also attributed to the nucleation of the dispersed phase of TPS (Cai et al., 2014). The Tc of the samples (Table 2) shows a temperature decrease from 135 to 100 °C in W1, which was reflected on the weeks of biodegradation. This temperature, in comparison with that of PLA, is correlated with the TGA and FTIR results, where structural changes in the film were observed during the biodegradation process. A single endothermic peak for melting at 170 °C was observed in all weeks. Additionally, all PLA/TPS blends showed an increase in the intensity of the endothermal peak attributed to the laminar arrangement and polymorphism of the PLA's crystalline structure (Anakabe et al., 2017).

The diffusion coefficient of water in an amorphous or semi-crystalline polymer is related to the molecular dynamics of its amorphous regions (Shogren et al., 2003). If the temperature of an amorphous system (polymer-water) is above the glass transition temperature, the movement will be rapid, the free volume will increase, and the water vapor permeability will be high. Moisture penetration through the film may be due to cavities within the film that produce increased water vapor permeability, which has been linked to the two-phase morphology of PLA/TPS blends.

The isotherms show the behavior of the type I or S sigmoid form, which is indicative of physical adsorption in the

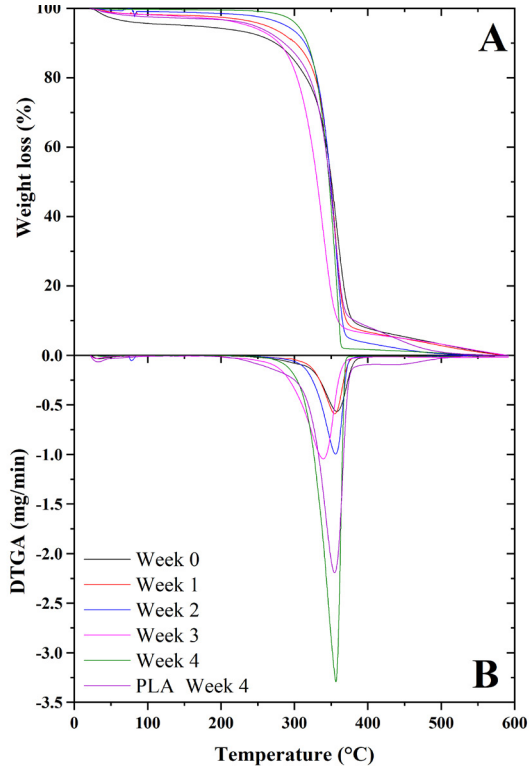

Figure 2. TGA (a) and DTG (b) curves for the biodegradation process of the TPS/PLA film
Source: Authors

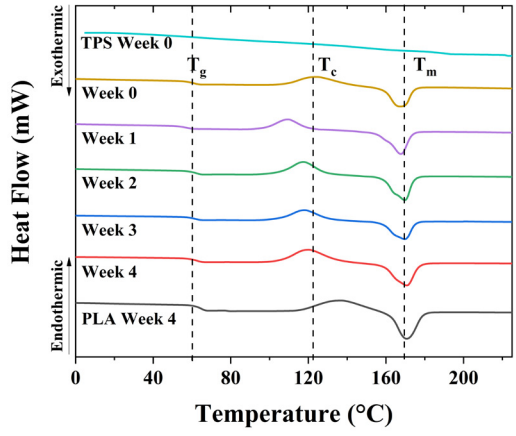

Figure 3. DSC curves for the biodegradation process of the TPS/PLA film
Source: Authors

multilayers of the material (Valsaraj, 2009). Table 3 shows the fit of the BET, GAB, Oswin, and Hasley models evaluated at different temperatures; it is evident that the model that best fits the data (MSE < 0,01) is BET, with R_{adj2} of 0,96804 at 10 °C, 0,95219 at 25 °C, and 0,97449 at 35 °C. From the prediction of the BET and GAB models, the amount of water that is strongly absorbed in the active sites of the film can be highlighted and is considered as the value at which the TPS/PLA mixture is most stable during storage (Chen et al., 2008; F. Wang et al., 2020). The addition of PLA in the blend provides a water vapor barrier, and TPS provides favorable water adsorption properties for the biodegradation

process. This is because starch is hydrophilic, unlike PLA, which tends to be completely hydrophobic (Sedničková et al., 2018). Therefore, it is possible that, in the film (TPS/PLA), the PLA prevents the starch from swelling, limiting the movement of the molecules and thus providing a part of the resistance to water permeability (Gürler et al., 2020). The variation in the water adsorption of TPS/PLA blends can be attributed to the behavior caused by the transition from the less ordered structure of starch to a higher-order structure that contains less water molecules (Lendvai et al., 2019). Consequently, the 3 300 cm^{-1} band is attributed to the stretching of the free inter- and intramolecular hydroxyl (-OH) groups of the starch chains, while the TPS exhibits a decrease in its intensity due to the interaction that occurs between starch and plasticizer by thermoplasticization (Altayan et al., 2017), which is due, in turn, to a greater interaction of the plasticizer with the polymeric chains of starch (Zdanowicz et al., 2019). On the other hand, in the region between 1 200 and 900 cm^{-1}, a band at 1 016 cm^{-1} attributed to the C-O stretching of the C-O-C group of the starch anhydroglucose ring is observed (Esmaeili et al., 2017) which is a function of the PLA concentration. The 995 cm^{-1} band, sensitive to water, is related to the intramolecular hydrogen bonding of the hydroxyl at C6, which can significantly decrease with increasing PLA.

Table 3. Water activity (a_w) models evaluated at different temperatures for a TPS/PLA blend

T (°C)	Model	Variable	Value	Standard Error	R^2_{adj}	MSE
10	BET	*a*	0,66208	0,04957	0,96804	0,00386
		b	0,11963			
	GAB	*k*	0,93128	0,06675	0,94206	0,01269
		a	-0,08992			
		b	-0,64516			
	Hasley	*a*	0,11001	0,04530	0,97331	0,00269
		b	0,81681			
	Oswin	*a*	0,09264	0,04827	0,96970	0,00347
		b	1,10053			
20	BET	*a*	0,660826	0,05011	0,95219	0,00571
		b	0,133906			
	GAB	*k*	1,03962	0,06258	0,92542	0,01416
		a	3,75515			
		b	0,05023			
	Hasley	*a*	0,119695	0,04987	0,95264	0,00571
		b	0,863831			
	Oswin	*a*	0,111984	0,05018	0,95204	0,00585
		b	1,059789			
35	BET	*a*	0,03633	0,04168	0,97449	0,00082
		b	1,056755			
	GAB	*k*	0,92990	0,04432	0.97115	0,02079
		a	3,62135			
		b	0,07296			
	Hasley	*a*	0,132909	0,04178	0,97436	0,00335
		b	0,906466			
	Oswin	*a*	0,143029	0,07425	0,91904	0,00264
		b	0,995217			

Source: Authors

This behavior has been reported by other authors working with hydrophilic polymers that have been plasticized with polyols, and it is associated with the increase in the amount of hydroxyl groups in the plasticizer. This increase causes an increase in the hygroscopicity of the material, reflected on the increase in the solubility coefficient of the samples with higher plasticizer concentration. Other authors have reported that a lower water vapor permeability is related to a lower value of the diffusion coefficient. They have also reported that the solubility coefficients of TPS/PLA blends are lower than those of TPS. This behavior is associated with a lower amount of hydroxyl groups in the blend that are available for interaction as the PLA concentration increases, which is in turn associated with the fact that each D-glucose repeat unit contains three of these groups, whereas PLA has two in each polymeric chain (Müller et al., 2012; Abdillahi et al., 2013). It is important to highlight, as mentioned by other authors (Hu and Vuillaume, 2020), that the increase in crystallinity increases the water vapor permeability in the film structure formed by PLA/TPS. This statement is validated by the data shown in the FTIR, DSC, and SEM analyses. Therefore, the incorporation of starch in these blends not only lowers the cost of the material but also contributes to its rapid biodegradation.

Biodegradation analysis

The results observed can be attributed to the dynamics of material degradation (Figure 4). Cellulose obtained a biodegradation percentage of 84%, the samples of the TPS/PLA blend 68%, and PLA 32% in 35 days. These results show that the test performed under the ASTM D5988 standard (ASTM International, 2018) is valid because there is a >20% difference between the control sample and the evaluated blend.

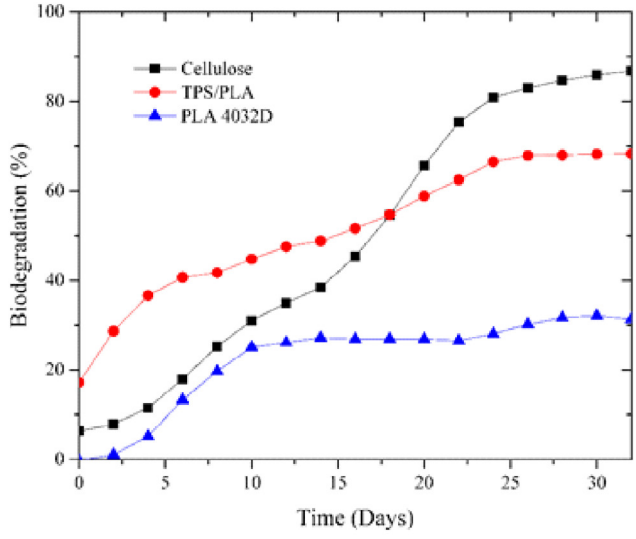

Figure 4. Biodegradability of the TPS/PLA film
Source: Authors

The reason for this is that biodegradation generally proceeds faster in the amorphous part of the polymer when compared to the crystalline ones, and the degradation rate

of polymers with higher molecular weight (PLA) is expected to be lower in comparison with shorter macromolecules (TPS), which are more easily digested by microorganisms. Consequently, the portion of PLA present in the TPS/PLA blended film containing a 72/28 ratio became more biodegradable than pure PLA (Sedničková, et al., 2018). These results are similar to those of Šerá et al., (2020), who found that cellulose obtained 91,4% of biodegradation of (25 °C) after 270 days, and a PBT/PLA mixture showed a percentage of 64,4%. These results are consistent with the biodegradation test performed under aerobic composting conditions, in which a 72% biodegradation percentage was found for a TPS/PLA film mixture (Bher, Auras, et al., 2018; Bher et al., 2019; Salazar-Sánchez et al., 2019). According to the results, the semi-crystalline PLA present in the mixture (TPS/PLA) reduces the amorphous regions in such a way that the molecular weight increases significantly and the crystalline regions start to decrease (Karamanlioglu and Robson, 2013; Middleton and Tipton, 2000; Weir et al., 2004), thus causing the fragmentation and disintegration of the material, as observed in the FTIR spectra and SEM micrographs, by means of the modifications to the film surface that could be noticed during the experiment. These results are similar to those reported by Olewnik-Kruszkowska et al. (2020), and they stem from the mineralization effect of the possible hydrolytic processes of microbial origin in the soil.

Scanning electron microscopy (SEM) analysis

The surface changes of the TPS/PLA blends during soil degradation (Figure 5) show that the film surfaces were smooth before degradation, and, after degrading under soil conditions during the evaluation time, they became rough; depressions and scratches appeared on the surface of these blends, similar to that reported by Lv et al. (2018) and Lv, Gu et al. (2017) for samples of 306D PLA and corn starch. After 30 days, there were fractures on the surface of each sample, cracks that would lead to the loss of mechanical strength. There were morphological changes regarding the color and shape of the film surface, which resulted from the attack of microorganisms to the PLA/TPS films (60:40) (Phetwarotai et al., 2013).

Conclusions

The addition of PLA and TPS is synergistic and significantly contributes to preservation and biodegradation processes by means of increasing or decreasing the crystallinity due to the number of amorphous phases present in the polymer. The biodegradability of the blends was confirmed by weight loss measurements with exposure time in the soil process. TPS accelerates the biodegradability of the blends in this medium due to its accessibility to microorganisms, its hydrophilic properties, and its amylose composition, which can be degraded more rapidly. The materials obtained from mixtures of TPS and PLA provide an additional advantage derived from the use of renewable sources for their manufacturing, as they provide the mixture with hydrophilic and biodegradable properties. This is an advantage over conventional plastics that must be exploited in order to obtain resistant materials which can be used in a similar way to conventional polymers.

Acknowledgements

We would like to thank the Young Researchers program of InnovAcción Cauca and Universidad del Cauca for funding project ID No. 4563, to which this research belongs.

References

Abdillahi, H., Chabrat, E., Rouilly, A., and Rigal, L. (2013). Influence of citric acid on thermoplastic wheat flour/poly(lactic acid) blends. II. Barrier properties and water vapor sorption isotherms. *Industrial Crops and Products, 50*, 104-111. https://doi.org/10.1016/j.indcrop.2013.06.028

Aguerre, R. J., Suárez, C., and Viollaz, P. E. (1989). New BET type multilayer sorption isotherms. *Lebensmittel-Wissenschaft & Technologie*, *22*, 192-195.

Altayan, M. M., Al Darouich, T., and Karabet, F. (2017). On the plasticization process of potato starch: Preparation and characterization. *Food Biophysics, 12*(4), 397-403. https://doi.org/10.1007/s11483-017-9495-2

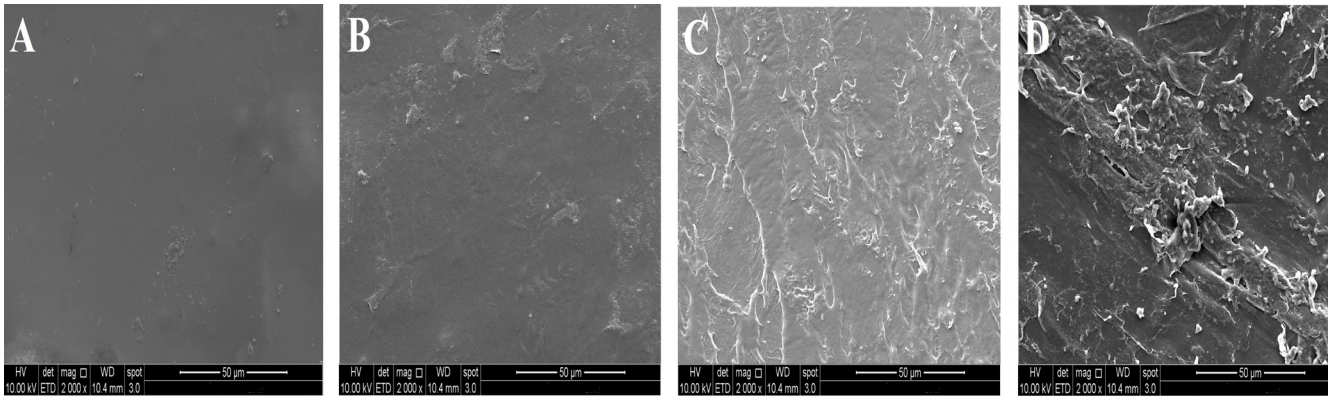

Figure 5. Surface changes in starch/PLA blends during soil degradation
Source: Authors

Anakabe, J., Zaldua Huici, A. M., Eceiza, A., Arbelaiz, A., and Avérous, L. (2017). Combined effect of nucleating agent and plasticizer on the crystallization behaviour of polylactide. *Polymer Bulletin, 74*(12), 4857-4886. https://doi.org/10.1007/s00289-017-1989-z

Anderson, R. B. (1946). Modifications of the Brunauer, Emmett and Teller Equation. *Journal of the American Chemical Society, 68*(4), 686-691. https://doi.org/10.1021/ja01208a049

Andrade, R. D. P., Roberto, L. M., and Pérez, C. E. C. (2011). Models of sorption isotherms for food: Uses and limitations. *Vitae, 18*(3), 325-334. https://revistas.udea.edu.co/index.php/vitae/article/view/10682

Arslan-Tontul, S. (2020). Moisture sorption isotherm, isosteric heat and adsorption surface area of whole chia seeds. *Lwt, 119*, 108859. https://doi.org/10.1016/j.lwt.2019.108859

ASTM International (2013). ASTM E1252-98: Standard practice for general techniques for obtaining infrared spectra for qualitative analysis. ASTM International.

ASTM International (2015). *ASTM D3418-15: Standard test method for transition temperatures and enthalpies of fusion and crystallization of polymers by differential scanning calorimetry*. ASTM International.

ASTM International (2018). *ASTM D5988-18: Standard test method for determining aerobic biodegradation of plastic materials in soil*. ASTM International.

ASTM International (2020). *ASTM E1131-20: Standard test method for compositional analysis by thermogravimetry*. ASTM International.

Bher, A., Auras, R., and Schvezov, C. E. (2018). Improving the toughening in poly(lactic acid)-thermoplastic cassava starch reactive blends. *Journal of Applied Polymer Science, 135*(15), 46140. https://doi.org/10.1002/app.46140

Bher, A., Unalan, I. U., Auras, R., Rubino, M., and Schvezov, C. E. (2018). Toughening of poly(lactic acid) and thermoplastic cassava starch reactive blends using graphene nanoplatelets. *Polymers, 10*(1), 95. https://doi.org/10.3390/polym10010095

Bher, A., Unalan, I. U., Auras, R., Rubino, M., and Schvezov, C. E. (2019). Graphene modifies the biodegradation of poly(lactic acid)-thermoplastic cassava starch reactive blend films. *Polymer Degradation and Stability, 164*, 187-197. https://doi.org/10.1016/j.polymdegradstab.2019.04.014

Brunauer, S., Emmett, P. H., and Teller, E. (1938). Adsorption of gases in multimolecular layers. *Journal of the American Chemical Society, 60*(2), 309-319. https://doi.org/10.1021/ja01269a023

Cai, J., Xiong, Z., Zhou, M., Tan, J., Zeng, F., Meihuma, Lin, S., and Xiong, H. (2014). Thermal properties and crystallization behavior of thermoplastic starch/poly(ε-caprolactone) composites. *Carbohydrate Polymers, 102*(1), 746-754. https://doi.org/10.1016/j.carbpol.2013.10.095

Cao, C., Shen, M., Hu, J., Qi, J., Xie, P., and Zhou, Y. (2020). Comparative study on the structure-properties relationships of native and debranched rice starch. *CyTA - Journal of Food, 18*(1), 84-93. https://doi.org/10.1080/19476337.2019.1710261

Carmona, V. B., Corrêa, A. C., Marconcini, J. M., and Mattoso, L. H. C. (2015). Properties of a biodegradable ternary blend of thermoplastic starch (TPS), poly(ε-caprolactone) (PCL) and poly(lactic acid) (PLA). *Journal of Polymers and the Environment, 23*(1), 83-89. https://doi.org/10.1007/s10924-014-0666-7

Castro-Aguirre, E., Auras, R., Selke, S., Rubino, M., and Marsh, T. (2018). Enhancing the biodegradation rate of poly(lactic acid) films and PLA bio-nanocomposites in simulated composting through bioaugmentation. *Polymer Degradation and Stability, 154*, 46-54. https://doi.org/10.1016/j.polymdegradstab.2018.05.017

Chen, C. H., and Lai, L. S. (2008). Mechanical and water vapor barrier properties of tapioca starch/decolorized hsian-tsao leaf gum films in the presence of plasticizer. *Food Hydrocolloids, 22*(8), 1584-1595. https://doi.org/10.1016/j.foodhyd.2007.11.006

Daza, L. D., Homez-Jara, A., Solanilla, J. F., and Váquiro, H. A. (2018). Effects of temperature, starch concentration, and plasticizer concentration on the physical properties of ulluco (Ullucus tuberosus Caldas)-based edible films. *International Journal of Biological Macromolecules, 120*(Part B), 1834-1845. https://doi.org/10.1016/j.ijbiomac.2018.09.211

American Public Health Association (APHA) (1999). *Standard methods for the examination of water and waste water* (20th ed.). APHA.

de Boer, J. H. (1953). The dynamical character of adsorption. *Soil Science, 76*(2), 166. https://doi.org/10.1097/00010694-195308000-00014

de Oliveira, T. A., Barbosa, R., Mesquita, A. B. S., Ferreira, J. H. L., de Carvalho, L. H., and Alves, T. S. (2019). Fungal degradation of reprocessed PP/PBAT/thermoplastic starch blends. *Journal of Materials Research and Technology, 9*(2), 2338-2349. https://doi.org/10.1016/j.jmrt.2019.12.065

de Oliveira, T. A., de Oliveira Mota, I., Mousinho, F. E. P., Barbosa, R., de Carvalho, L. H., and Alves, T. S. (2019). Biodegradation of mulch films from poly(butylene adipate co-terephthalate), carnauba wax, and sugarcane residue. *Journal of Applied Polymer Science, 136*(47), 48240. https://doi.org/10.1002/app.48240

Dutcher, C. S., Ge, X., Wexler, A. S., and Clegg, S. L. (2011). Statistical mechanics of multilayer sorption: Extension of the Brunauer-Emmett-Teller (BET) and Guggenheim-Anderson-de Boer (GAB) adsorption isotherms. *Journal of Physical Chemistry C, 115*(33), 16474-16487. https://doi.org/10.1021/jp203879d

Esmaeili, M., Pircheraghi, G., Bagheri, R., and Altstädt, V. (2019). Poly(lactic acid)/coplasticized thermoplastic starch blend: Effect of plasticizer migration on rheological and mechanical properties. *Polymers for Advanced Technologies, 30*(4), 839-851. https://doi.org/10.1002/pat.4517

Frone, A. N., Berlioz, S., Chailan, J. F., and Panaitescu, D. M. (2013). Morphology and thermal properties of PLA-cellulose nanofibers composites. *Carbohydrate Polymers, 91*(1), 377-384. https://doi.org/10.1016/j.carbpol.2012.08.054

Garalde, R. A., Thipmanee, R., Jariyasakoolroj, P., and Sane, A. (2019). The effects of blend ratio and storage time on thermoplastic starch/poly(butylene adipate-co-terephthalate) films. *Heliyon, 5*(3), e01251. https://doi.org/10.1016/j.heliyon.2019.e01251

Gopi, S., Amalraj, A., Jude, S., Thomas, S., and Guo, Q. (2019). Bionanocomposite films based on potato, tapioca starch

and chitosan reinforced with cellulose nanofiber isolated from turmeric spent. *Journal of the Taiwan Institute of Chemical Engineers, 96*, 664-671. https://doi.org/10.1016/j.jtice.2019.01.003

Guggenheim, E. A. (1966). *Applications of statistical mechanics*. Clarendon Press.

Halsey, G. (1948). Physical adsorption on non-uniform surfaces. *The Journal of Chemical Physics, 16*(10), 931-937. https://doi.org/10.1063/1.1746689

Gürler, N., Paşa, S., Hakkı Alma, M., and Temel, H. (2020). The fabrication of bilayer polylactic acid films from cross-linked starch as eco-friendly biodegradable materials: Synthesis, characterization, mechanical and physical properties. *European Polymer Journal, 127*, 109588. https://doi.org/10.1016/j.eurpolymj.2020.109588

Heidemann, H. M., Dotto, M. E. R., Laurindo, J. B., Carciofi, B. A. M., and Costa, C. (2019). Cold plasma treatment to improve the adhesion of cassava starch films onto PCL and PLA surface. *Colloids and Surfaces A: Physicochemical and Engineering Aspects, 580*, 123739 https://doi.org/10.1016/j.colsurfa.2019.123739

Homez, A. K., Daza, L. D., Solanilla, J. F., and Váquiro, H. A. (2018). Effect of temperature, starch and plasticizer concentrations on color parameters of ulluco (Ullucus tuberosus Caldas) edible films. *IOP Conference Series: Materials Science and Engineering, 437*, 012003. https://doi.org/10.1088/1757-899X/437/1/012003

Hu, L., and Vuillaume, P. Y. (2020). Reactive compatibilization of polymer blends by coupling agents and interchange catalysts. In A. R. Ajitha and T. Thomas (Eds.), *Compatibilization of Polymer Blends* (pp. 205-248). Elsevier. https://doi.org/10.1016/b978-0-12-816006-0.00007-4

Iglesias, H. A., and Chirife, J. (1995). An alternative to the Guggenheim, Anderson and De Boer model for the mathematical description of moisture sorption isotherms of foods. *Food Research International, 28*(3), 317-321. https://doi.org/10.1016/0963-9969(94)00002-P

ISO (2012). *10210:2012. Plastics -- Methods for the preparation of samples for biodegradation testing of plastic materials*. https://www.iso.org/standard/45851.html

Karamanlioglu, M., and Robson, G. D. (2013). The influence of biotic and abiotic factors on the rate of degradation of poly(lactic) acid (PLA) coupons buried in compost and soil. *Polymer Degradation and Stability, 98*(10), 2063-2071. https://doi.org/10.1016/j.polymdegradstab.2013.07.004

Lambert, S., and Wagner, M. (2017). Environmental performance of bio-based and biodegradable plastics: The road ahead. *Chemical Society Reviews, 46*(22), 6855-6871. https://doi.org/10.1039/c7cs00149e

Lambert, T., and Perga, M. E. (2019). Non-conservative patterns of dissolved organic matter degradation when and where lake water mixes. *Aquatic Sciences, 81*(4), 64. https://doi.org/10.1007/s00027-019-0662-z

Lendvai, L., Sajó, I., and Karger-Kocsis, J. (2019). Effect of storage time on the structure and mechanical properties of starch/bentonite nanocomposites. *Starch, 71*(1-2), 1800123. https://doi.org/10.1002/star.201800123

Li, Y., Zhang, K., Nie, M., and Wang, Q. (2020). Application of compatibilized polymer blends in packaging. In A. R. Ajitha and T. Thomas (Eds.), *Compatibilization of Polymer Blends* (pp. 539-561). Elsevier. https://doi.org/10.1016/b978-0-12-816006-0.00019-0

Liu, H., Chaudhary, D., Yusa, S. I., and Tadé, M. O. (2011). Glycerol/starch/Na+-montmorillonite nanocomposites: A XRD, FTIR, DSC and 1H NMR study. *Carbohydrate Polymers, 83*(4), 1591-1597. https://doi.org/10.1016/j.carbpol.2010.10.018

Lv, S., Gu, J., Tan, H., and Zhang, Y. (2017). The morphology, rheological, and mechanical properties of wood flour/starch/poly(lactic acid) blends. *Journal of Applied Polymer Science, 134*(16), 44743. https://doi.org/10.1002/app.44743

Lv, S., Zhang, Y., Gu, J., and Tan, H. (2017). Biodegradation behavior and modelling of soil burial effect on degradation rate of PLA blended with starch and wood flour. *Colloids and Surfaces B: Biointerfaces*, *159*, 800-808. https://doi.org/10.1016/j.colsurfb.2017.08.056

Lv, S., Zhang, Y., Gu, J., and Tan, H. (2018). Physicochemical evolutions of starch/poly (lactic acid) composite biodegraded in real soil. *Journal of Environmental Management, 228*, 223-231. https://doi.org/10.1016/j.jenvman.2018.09.033

Middleton, J. C., and Tipton, A. J. (2000). Synthetic biodegradable polymers as orthopedic devices. *Biomaterials, 21*(23), 2335-2346. https://doi.org/10.1016/S0142-9612(00)00101-0

Mierzwa-Hersztek, M., Gondek, K., and Kopeć, M. (2019). Degradation of polyethylene and biocomponent-derived polymer materials: An overview. *Journal of Polymers and the Environment, 27*(3), 600-611. https://doi.org/10.1007/s10924-019-01368-4

Müller, C. M. O., Pires, A. T. N., and Yamashita, F. (2012). Characterization of thermoplastic starch/poly(lactic acid) blends obtained by extrusion and thermopressing. *Journal of the Brazilian Chemical Society, 23*(3), 426-434. https://doi.org/10.1590/S0103-50532012000300008

Müller, J., González-Martínez, C., and Chiralt, A. (2017). Poly(lactic) acid (PLA) and starch bilayer films, containing cinnamaldehyde, obtained by compression moulding. *European Polymer Journal, 95*, 56-70. https://doi.org/10.1016/j.eurpolymj.2017.07.019

Nasseri, R., Ngunjiri, R., Moresoli, C., Yu, A., Yuan, Z., and Xu, C. (Charles). (2020). Poly(lactic acid)/acetylated starch blends: Effect of starch acetylation on the material properties. *Carbohydrate Polymers, 229*, 115453. https://doi.org/10.1016/j.carbpol.2019.115453

Nevoralová, M., Koutný, M., Ujčić, A., Horák, P., Kredatusová, J., Šerá, J., Růžek, L., Růžková, M., Krejčíková, S., Šlouf, M., and Kruliš, Z. (2019). Controlled biodegradability of functionalized thermoplastic starch based materials. *Polymer Degradation and Stability, 170*, 108995. https://doi.org/10.1016/j.polymdegradstab.2019.108995

Olewnik-Kruszkowska, E., Burkowska-But, A., Tarach, I., Walczak, M., and Jakubowska, E. (2020). Biodegradation of polylactide-based composites with an addition of a compatibilizing agent in different environments. *International Biodeterioration and Biodegradation, 147*, 104840. https://doi.org/10.1016/j.ibiod.2019.104840

Oswin, C. R. (1946). The kinetics of package life. III. The isotherm. *Journal of the Society of Chemical Industry, 65*(12), 419-421. https://doi.org/10.1002/jctb.5000651216

Özeren, H. D., Olsson, R. T., Nilsson, F., and Hedenqvist, M. S. (2020). Prediction of plasticization in a real biopolymer system (starch) using molecular dynamics simulations. *Materials & Design, 187*, 108387. https://doi.org/10.1016/j.matdes.2019.108387

Palai, B., Biswal, M., Mohanty, S., and Nayak, S. K. (2019). In situ reactive compatibilization of polylactic acid (PLA) and thermoplastic starch (TPS) blends; synthesis and evaluation of extrusion blown films thereof. *Industrial Crops and Products, 141*, 111748. https://doi.org/10.1016/j.indcrop.2019.111748

Pattanasuttichonlakul, W., Sombatsompop, N., and Prapagdee, B. (2018). Accelerating biodegradation of PLA using microbial consortium from dairy wastewater sludge combined with PLA-degrading bacterium. *International Biodeterioration and Biodegradation, 132*, 74-83. https://doi.org/10.1016/j.ibiod.2018.05.014

Phetwarotai, W., Potiyaraj, P., and Aht-Ong, D. (2013). Biodegradation of polylactide and gelatinized starch blend films under controlled soil burial conditions. *Journal of Polymers and the Environment, 21*(1), 95-107. https://doi.org/10.1007/s10924-012-0530-6

Riba, J. R., Cantero, R., García-Masabet, V., Cailloux, J., Canals, T., and Maspoch, M. L. (2020). Multivariate identification of extruded PLA samples from the infrared spectrum. *Journal of Materials Science, 55*(3), 1269-1279. https://doi.org/10.1007/s10853-019-04091-6

Salazar-Sánchez, M. del R., Campo-Erazo, S. D., Villada-Castillo, H. S., and Solanilla-Duque, J. F. (2019). Structural changes of cassava starch and polylactic acid films submitted to biodegradation process. *International Journal of Biological Macromolecules, 129*, 442-447. https://doi.org/10.1016/j.ijbiomac.2019.01.187

Salazar-Sánchez, M. D. R., Cañas-Montoya, J. A., Villada-Castillo, H. S., Solanilla-Duque, J. F., Rodríguez-Herrera, R., and Avalos-Belmotes, F. (2020). Biogenerated polymers: An enviromental alternative. *DYNA, 87*(214), 75-84. https://doi.org/10.15446/dyna.v87n214.82163

Sedničková, M., Pekařová, S., Kucharczyk, P., Bočkaj, J., Janigová, I., Kleinová, A., Jochec-Mošková, D., Omaníková, L., Perdochová, D., Koutný, M., Sedlařík, V., Alexy, P., and Chodák, I. (2018). Changes of physical properties of PLA-based blends during early stage of biodegradation in compost. *International Journal of Biological Macromolecules, 113*, 434-442. https://doi.org/10.1016/j.ijbiomac.2018.02.078

Šerá, J., Serbruyns, L., de Wilde, B., and Koutný, M. (2020). Accelerated biodegradation testing of slowly degradable polyesters in soil. *Polymer Degradation and Stability, 171*, 109031. https://doi.org/10.1016/j.polymdegradstab.2019.109031

Shogren, R. L., Doane, W. M., Garlotta, D., Lawton, J. W., and Willett, J. L. (2003). Biodegradation of starch/polylactic acid/poly(hydroxyester-ether) composite bars in soil. *Polymer Degradation and Stability, 79*(3), 405-411. https://doi.org/10.1016/S0141-3910(02)00356-7

SSLMM-42-2-92. Soil Survey Laboratory Methods Manual Reporte No.42, Versión 2.0, 1992

Torres, M. D., Moreira, R., Chenlo, F., and Vázquez, M. J. (2012). Water adsorption isotherms of carboxymethyl cellulose, guar, locust bean, tragacanth and xanthan gums. *Carbohydrate Polymers, 89*(2), 592-598. https://doi.org/10.1016/j.carbpol.2012.03.055

Valsaraj, K. T. (2009). *Elements of environmental engineering: Thermodynamics and kinetics*. Taylor & Francis Group.

van den Berg, C. (1981). *Vapour sorption equilibria and other Water-starch interactions; A Physico-chemical approach* [Doctoral dissertation, Wageningen University]. http://library.wur.nl/WebQuery/wurpubs/75143

Wang, F., Lei, S., Ou, J., Li, C., and Li, W. (2019). Novel All-Natural Material for Oil/Water Separation. *Industrial & Engineering Chemistry Research, 58*(5), 1924-1931. https://doi.org/10.1021/acs.iecr.8b05535

Wang, P., Xiong, Z., Fei, P., Cai, J., Walayat, N., and Xiong, H. (2020). An approach for compatibilization of the starch with poly(lactic acid) and ethylene-vinyl acetate-glycidyl-methacrylate. *International Journal of Biological Macromolecules, 161*, 44-58. https://doi.org/10.1016/j.ijbiomac.2020.06.011

Wang, H., Wu, J., Luo, S., Zou, P., Guo, B., Liu, Y., Chen, J., and Liu, C. (2020). Improving instant properties of kudzu powder by extrusion treatment and its related mechanism. *Food Hydrocolloids, 101*, 105475. https://doi.org/10.1016/j.foodhyd.2019.105475

Weir, N. A., Buchanan, F. J., Orr, J. F., and Dickson, G. R. (2004). Degradation of poly-L-lactide. Part 1: In vitro and in vivo physiological temperature degradation. *Proceedings of the Institution of Mechanical Engineers, Part H: Journal of Engineering in Medicine, 218*(5), 307-319. https://doi.org/10.1243/0954411041932782

Zdanowicz, M., Staciwa, P., Jędrzejewski, R., and Spychaj, T. (2019). Sugar alcohol-based deep eutectic solvents as potato starch plasticizers. *Polymers, 11*(9), 1385. https://doi.org/10.3390/polym11091385